JHEP

Published for SISSA by Springer

Received: January 4, 2018
Revised: May 24, 2018
Accepted: June 15, 2018
Published: July 2, 2018

Multi-photon production in the Type-I 2HDM

A. Arhrib,[a] **R. Benbrik,**[b,c] **S. Moretti,**[d] **A. Rouchad,**[b] **Q.-S. Yan**[e,f] **and Xianhui Zhang**[f]

[a] *Faculté des Sciences et Techniques, Abdelmalek Essaadi University, B.P. 416, Tangier, Morocco*
[b] *LPHEA, Semlalia, Cadi Ayyad University, Marrakech, Morocco*
[c] *MSISM Team, Faculté Polydisciplinaire de Safi, Sidi Bouzid, BP 4162, Safi, Morocco*
[d] *School of Physics and Astronomy, University of Southampton, Southampton, SO17 1BJ, United Kingdom*
[e] *School of Physics Sciences, University of Chinese, Academy of Sciences, Beijing 100039, P.R. China*
[f] *Center for Future High Energy Physics, Chinese Academy of Sciences, Beijing 100039, P.R. China*

E-mail: aarhrib@gmail.com, r.benbrik@uca.ac.ma, s.moretti@soton.ac.uk, abdessamad.rouchad@edu.uca.ac.ma, yanqishu@ucas.ac.cn, xianhuizhang@ucas.ac.cn

Abstract: This paper presents a study of a possible contribution to a Higgs boson signal in the $hh \to \gamma\gamma\gamma\gamma$ channel due to $H \to hh$ decays, in the framework of the CP-conserving 2-Higgs Doublet Model Type-I (2HDM-I), where the heavier of the two CP-even Higgs bosons defined herein, H, is the SM-like Higgs state observed with a mass of 125 GeV at the Large Hadron Collider (LHC). We perform a broad scan of the 2HDM-I parameter space, in presence of both up-to-date theoretical and experimental constraints, in order to extract the interesting regions yielding such a signal. Then, after validating our numerical framework against public experimental analyses carried out at the LHC, we proceed to assess its scope in constraining and/or extracting the $gg \to H \to hh \to \gamma\gamma\gamma\gamma$ signal in presence of a sophisticated Monte Carlo (MC) simulation. We find that, over a substantial region of the 2HDM-I parameter space presently un-accessible, the LHC will be able to establish such a potential signature in the next 2–3 years.

Keywords: Beyond Standard Model, Higgs Physics

ArXiv ePrint: 1712.05332

https://doi.org/10.1007/JHEP07(2018)007

JHEP07(2018)007

Contents

1 Introduction

Following the discovery of a Higgs boson with a mass of 125 GeV [1, 2], henceforth labeled by H, with characteristics similar to those of the predicted state of the Standard Model (SM), experiments at the LHC have effectively begun to probe Electro-Weak Symmetry Breaking (EWSB) dynamics. The search channel that mostly enabled discovery was the one involving $gg \to H$ production followed by a $H \to \gamma\gamma$ decay, thanks to its cleanliness in the hadronic environment of the LHC and the sharp resolution in the di-photon invariant mass achievable by the LHC detectors, despite this decay being actually very subleading. Other Higgs signals were eventually established and studied in detail in order to measure the H state fundamental parameters, i.e., mass, width and couplings, all broadly consistent with the SM picture. Furthermore, comprehensive analyses investigating the spin and parity of the discovered particle have finally confirmed its most likely spin-0 and Charge/Parity (CP)-even nature, again, well in line with SM predictions.

The EWSB dynamics implemented within the SM is minimal in nature, allowing for the existence of only one Higgs boson. However, this needs not be the preferred realisation chosen by Nature. Just like the gauge and Yukawa sectors are not, i.e., there are multiple spin-1 and spin-1/2 states, there is a case for conceiving the possibility of an extended spin-0 sector too. As the Higgs boson so far discovered emerges from a doublet representation, a meaningful approach to surpass the SM is exemplified by 2HDMs [3–6], wherein a second (complex) Higgs doublet is added to the fundamental field representations of the SM. Upon EWSB, this yields five Higgs boson states as physical objects: two neutral CP-even ones (h and H with, conventionally, $m_H > m_h$), one neutral CP-odd one (A) and two charged ones ($H^\pm$) [7].

In the light of the established nature of the Higgs boson signals at the LHC, as mentioned above, in terms of its mass, width, couplings, spin and CP state, there exists therefore the possibility that in a 2HDM the observed SM-like Higgs state can be either the

JHEP07(2018)007

h [8, 9] or H [10, 11] one. An intriguing possibility is that Nature made the second choice, i.e., the heavy 2HDM CP-even state, so that a pair of the light ones could appear as its decay products, as the Hhh vertex is indeed allowed by the most general 2HDM scalar potential and underlying symmetries, which in fact coincide with those of the SM, except (possibly) for an additional Z_2 one introduced to prevent (large) Flavour Changing Neutral Currents (FCNCs) [12, 13] that may otherwise emerge in presence of a 2HDM (pseudo)scalar sector. Such a mass hierarchy, i.e., $m_H > 2m_h$, can easily be realised over the parameter space of one particular realisation of a 2HDM, so-called Type-I (2HDM-I), see next section for details, which in fact allows for h masses down to even 20–30 GeV, well compatible with both theoretical and experimental constraints.

However, the requirement that one out of h or H has physical properties consistent with the observed Higgs boson state puts rather stringent bounds on the 2HDM parameter space. For example, it is well known that, in a 2HDM, there exists a 'decoupling limit', where $m_{H,A,H^\pm} \gg m_Z$, $\cos(\beta-\alpha) \approx 0$ [7] and the couplings of the h state to the SM particles are identical to those of the SM Higgs boson. Alternatively, a 2HDM also possesses an 'alignment limit', in which either one of h [8, 9] or H [10, 11] can mimic the SM Higgs boson. This is a welcome feature, as we will be working in a configuration of the 2HDM-I [14] parameter space close to the alignment limit realised through the H state, however, we will specifically be concentrating on those parameters which enable the h state to be (nearly) fermiophobic, so that the $h \to \gamma\gamma$ decay (mediated by $W^\pm$ and $H^\pm$ boson loops) can be dominant.

Hence, all this opens up the possibility of a rather spectacular 2HDM-I signal, in the form of the following production and (cascade) decay process, $gg \to H \to hh \to \gamma\gamma\gamma\gamma$, indeed relying upon the aforementioned characteristic of photonic signals in the LHC detectors. Clearly, the presence of two Higgs bosons as intermediate states in such a signature induces a phase space suppression (with respect to the production of a single Higgs state), however, this can be well compensated by the fact that the $H \to hh$ transition is resonant and, as mentioned, di-photon decays of the h state can be dominant in the 2HDM-I [14] when occurring near its fermiophobic limit. Furthermore, the knowledge of the H mass (125 GeV in our scenario), combined with the ability of reconstructing in each event photon pairs with similar masses, the former thus enabling one to enforce the $m_{\gamma\gamma\gamma\gamma} \approx 125$ GeV requirement and the latter the $m_{\gamma\gamma} \approx m'_{\gamma\gamma}$ one, allows us to exploit two powerful kinematic handles in suppressing the background, again, bearing in mind the high mass resolutions achievable in photon mass reconstructions.

In the present study, in essence, we explore the discovery potential of a light scalar Higgs boson h of mass less than $m_H/2$ at the LHC Run 2 (hence with Center-of-Mass (CM) energy $\sqrt{s} = 13$ TeV and standard luminosity conditions), where — as explained — H represents the SM-like Higgs state [10, 11]. Chiefly, we consider the production of a light h pair indirectly via the decay

$$H \to hh, \tag{1.1}$$

with the production of H via the standard mechanisms, which are dominated by gluon-gluon fusion. In this connection, it is to be noted that the total Branching Ratio (BR) of

JHEP07(2018)007

the SM-like Higgs boson to undetected Beyond the SM (BSM) decay modes ($\mathrm{BR}_{\mathrm{BSM}}$) is restricted by current Higgs data and predicted to be [15]

$$\mathrm{BR}_{\mathrm{BSM}} \leq 0.34 \text{ at } 95\% \text{ Confidence Level (CL)}. \tag{1.2}$$

That is, the presence of non-SM decay modes of SM-like Higgs boson is not completely ruled out, which acts as a further motivation of our study.

In carrying out the latter, we borrow from existing experimental results. The ATLAS collaboration carried out searches for new phenomena in events with at least three photons at a CM energy of 8 TeV and with an integrated luminosity of $20.3\,\mathrm{fb}^{-1}$. From the non-observation of any excess, limits are set at 95% CL on the rate of the relevant signal events in terms of cross section multiplied by a suitable BR combination [16]

$$\sigma_{\mathrm{BSM}} \times \beta' \leq 10^{-3}\sigma_{\mathrm{SM}}, \tag{1.3}$$

where $\beta' = \mathrm{BR}(H \to AA) \times \mathrm{BR}(A \to \gamma\gamma)^2$, σ_{BSM} is the Higgs production cross section in a possible BSM scenario and σ_{SM} is the same, but for the SM Higgs. The above constraint sets an upper limit on β' as

$$\beta' \leq 10^{-3}, \tag{1.4}$$

provided the Higgs state H in the context of new physics phenomena is the SM-like Higgs boson of mass 125 GeV. In particular, we will validate a numerical toolbox that we have created to carry out a Monte Carlo (MC) analysis against results published therein for the case of $H \to AA$ decays and extrapolate them to the case of $H \to hh$ ones, which constitute the dominant four photon signal in our case.

The plan of the paper is as follows. In section 2, we introduce 2HDMs [3–6] in general and describe in particular our construct (the 2HDM-I [14]), including dwelling on the theoretical (see [17–27]) and experimental (see later on) constraints placed upon its parameter space. (Herein, we also comment on the fermiophobic limit of the 2HDM-I and its experimental status.) Section 3 is devoted to present our numerical results for the (inclusive) four photons cross section and to motivate the selection of our Benchmark Points (BPs). Then we move on to describe the numerical tools we have used and the MC analysis carried out, including illustrating our results for the exclusive cross section in section 4. We then conclude in section 5. Some technical details of our calculations are presented in appendices A and B.

2 The 2HDM-I and its fermiophobic limit

The 2HDM scalar potential. The most general 2HDM scalar potential which is $\mathrm{SU}(2)_L \otimes \mathrm{U}(1)_Y$ invariant with a softly broken Z_2 symmetry can be written as

$$\begin{aligned} V(\phi_1,\phi_2) = {} & m_{11}^2\phi_1^+\phi_1 + m_{22}^2\phi_2^+\phi_2 - \left[m_{12}^2\phi_1^+\phi_2 + \mathrm{h.c.}\right] \\ & + \frac{1}{2}\lambda_1(\phi_1^+\phi_1)^2 + \frac{1}{2}\lambda_2(\phi_2^+\phi_2)^2 + \lambda_3(\phi_1^+\phi_1)(\phi_2^+\phi_2) \\ & + \lambda_4(\phi_1^+\phi_2)(\phi_2^+\phi_1) + \left[\frac{1}{2}\lambda_5(\phi_1^+\phi_2)^2 + \mathrm{h.c.}\right], \end{aligned} \tag{2.1}$$

JHEP07(2018)007

where ϕ_1 and ϕ_2 have weak hypercharge $Y = +1$ while v_1 and v_2 are their respective Vacuum Expectation Values (VEVs). Through the minimisation conditions of the potential, m_{11}^2 and m_{22}^2 can be traded for v_1 and v_2 and the tree-level mass relations allow the quartic couplings λ_{1-5} to be substituted by the four physical Higgs boson masses and the neutral sector mixing term $\sin(\beta-\alpha)$, where β is defined through $\tan\beta = v_2/v_1$ and α is the mixing angle between the CP-even interaction states. Thus, in total, the Higgs sector of the 2HDM has 7 independent parameters, which include $\tan\beta$, $\sin(\beta-\alpha)$ (or α), m_{12}^2 and the four physical Higgs boson masses.

As explained in the Introduction, the 2HDM possesses two alignment limits: one with h SM-like [8, 9] and an other one with H SM-like [10, 11]. In the present study, we are interested in the alignment limit where H is the SM-like Higgs boson discovered at CERN, which implies that $\cos(\beta-\alpha) \approx 1$. Then, we take $m_h < m_H/2 \approx 62.5\,\text{GeV}$, so that the decay channel $H \to hh$ would always be open.

From the above scalar potential one can derive the following triple scalar couplings needed for our study:

$$\begin{aligned}
Hhh &= -\frac{1}{2}\frac{g c_{\beta-\alpha}}{m_W s_{2\beta}^2}\Big[(2m_h^2 + m_H^2)s_{2\alpha}s_{2\beta} - 2(3s_{2\alpha} - s_{2\beta})m_{12}^2\Big],\\
HAA &= -\frac{g}{2m_W s_{2\beta}^2}\Big[(2m_A^2 - m_H^2)s_{2\beta}^2 c_{\beta-\alpha} + 2m_H^2 s_{2\beta}s_{\beta+\alpha} - 4m_{12}^2 s_{\beta+\alpha}\Big],\\
hH^\pm H^\mp &= \frac{1}{2}\frac{g}{m_W s_{2\beta}^2}\Big[(m_h^2 - 2m_{H^\pm}^2)s_{\beta-\alpha}s_{2\beta}^2 - 2c_{\beta+\alpha}(m_h^2 s_{2\beta} - 2m_{12}^2)\Big],
\end{aligned} \tag{2.2}$$

where g is the SU(2) gauge coupling constant. We have used the notation s_x and c_x as short-hand for $\sin(x)$ and $\cos(x)$, respectively. It is clear from the above couplings that Hhh is proportional to $c_{\beta-\alpha}$ which is close to unity in our case and hence the $\text{BR}(H \to hh)$ would not be suppressed. Moreover, in the exact fermiophobic limit $\alpha \approx \pm\pi/2$ becomes proportional to m_{12}^2. The vertex HAA has two terms, one proportional to $c_{\beta-\alpha}$ and the other proportional to $s_{\beta+\alpha}$ which is close to c_β in the fermiophobic limit $\alpha \approx \pi/2$. Finally, the coupling $hH^\pm H^\mp$ can be large so as to contribute sizably to the $h \to \gamma\gamma$ decay rate.

Fermiophobic limit of the 2HDM-I. In general, in the 2HDM, both Higgs doublets can couple to quarks and leptons exactly as in the SM. However, in such case one has tree level FCNCs which would lead to large contribution to B-physics observables in conflict with data. In order to avoid this, the 2HDM needs to satisfy a discrete Z_2 symmetry [12, 13] which guarantees the absence of this phenomenon. Several type of 2HDMs exist depending on the Z_2 charge assignment of the Higgs doublets [13]. In our study, we will focus on the 2HDM-I. In this model only the doublet ϕ_2 couples to all the fermions as in the SM while ϕ_1 does not couple to any of the fermions.

The Yukawa interactions in terms of the neutral and charged Higgs mass eigenstates in a general 2HDM can be written as:

$$\begin{aligned}
-\mathcal{L}_{\text{Yukawa}}^{\text{2HDM}} &= \Sigma_{f=u,d,l}\frac{m_f}{v}\left(\xi_f^h \bar{f}fh + \xi_f^H \bar{f}fH - i\xi_f^A \bar{f}\gamma_5 fA\right)\\
&\quad + \left\{\frac{\sqrt{2}V_{ud}}{v}\bar{u}(m_u\xi_u^A P_L + m_d\xi_d^A P_R)dH^+ + \frac{\sqrt{2}m_l\xi_l^A}{v}\bar{\nu}_L l_R H^+ + \text{h.c.}\right\},
\end{aligned} \tag{2.3}$$

JHEP07(2018)007

where $v^2 = v_1^2 + v_2^2 = (2\sqrt{2}G_F)^{-1}$, V_{ud} is the top-left entry of the Cabibbo-Kobayashi-Maskawa (CKM) matrix and P_L and P_R are the left- and right-handed projection operators, respectively. In the 2HDM-I, we have

$$\begin{aligned} &\xi_f^h = \cos\alpha/\sin\beta \quad \text{and} \quad \xi_f^H = \sin\alpha/\sin\beta, \quad \text{for} \quad f = u, d, l, \\ &\xi_d^A = -\cot\beta\,, \qquad\qquad \xi_u^A = \cot\beta \qquad\quad \text{and} \quad \xi_l^A = -\cot\beta. \end{aligned} \tag{2.4}$$

From the above Lagrangian (2.3) and (2.4), it is clear that for $\alpha \approx \pm\frac{\pi}{2}$ the tree level coupling of the light CP-even Higgs h to quarks and leptons are very suppressed. Hence h is fermiophobic in this limit [28, 29]. Note that, in the 2HDM-I, the CP-odd Higgs coupling to fermions is proportional to $\cot\beta$ and hence would not be fermiophobic for any choice of $\tan\beta$. Since we are interested in the case where H is SM-like ($\cos(\beta-\alpha) \approx 1$) and $m_h \leq m_H/2 \approx 62.5\,\text{GeV}$, so that the decay $H \to hh$ is open, the main decays of the lightest Higgs state h are into the (tree level) channels $h \to V^*V^*$ and $h \to Z^*A$ when $m_A < m_h$, otherwise the (one loop) $h \to Z^*\gamma$, $h \to \gamma\gamma$ and (tree level) $h \to b\bar{b}$ ones are the most important modes in the fermiophobic limit for light m_h. Despite the $h \to b\bar{b}$ rate vanishes in the exact fermiophobic limit, it may be mediated at one loop level [31] through $W^\pm$, $H^\pm$ and neutral Higgs boson (h, H and A) loops. However, it was pointed out in [31] that the BR($h \to b\bar{b}$) at one loop can at most reach 10% for a small m_h:[1] see figure 1 for the properties of the $h \to b\bar{b}$ decay, also in relation to the $h \to \gamma\gamma$ one. (The formulae for the one loop $h \to b\bar{b}$ decay are found in appendix A.) Further, even in the totally fermiophobic limit, the h state can still decay into fermions via the two following channels: firstly, $h \to V^*V^*(\to f\bar{f}f'\bar{f}')$, which has two sources of suppression, i.e., the phase space one and the fact that $hVV \propto \sin(\beta-\alpha) \approx 0$, and, secondly, $h \to Z^*\gamma(\to f\bar{f}\gamma)$, which is both phase space and loop suppressed. Therefore, the decays $h \to \gamma\gamma$ and $h \to Z^*A$ ($m_A < m_h$) are expected to compete with each other and dominate in the fermiophobic limit. In fact, it is well known that $h \to \gamma\gamma$ is mediated by the $W^\pm$ loops which interfere destructively with the top and charged Higgs ones. In the limit where $\sin(\beta-\alpha) \to 0$, the $W^\pm$ loops vanish and only the top and charged Higgs ones contribute. When $\cos\alpha$ vanishes, the h state, with mass $\leq 62.5\,\text{GeV}$, becomes fermiophobic and consequently the BR($h \to \gamma\gamma$) can become 100% if $h \to Z^*A$ is not open. In contrast, the coupling hZA is proportional to $\cos(\beta-\alpha)$, which is close to unity in our scenario, therefore, when $h \to Z^*A$ is open for $m_A < m_h$, it dominates over $h \to \gamma\gamma$.

Fermiophobic Higgs bosons have been searched for at LEP and Tevatron. The LEP collaborations used $e^+e^- \to Z^* \to Zh$ followed by the decay $h \to \gamma\gamma$ and set a lower limit on m_h of the order 100 GeV [30, 33–35]. At the Tevatron, both Higgs-strahlung ($pp \to Vh$, $V = W^\pm, Z$) and vector boson fusion ($qq \to q'q'h$) have been used to search for fermiophobic Higgs decays of the type $h \to \gamma\gamma$ [36], with similar results to those obtained at LEP. Note that both LEP and Tevatron assumed a full SM coupling for hVV ($V = Z, W$) which would not be the case for the CP-even Higgs h in the 2HDM-I where $hVV \propto \sin(\beta-\alpha)$ can be very suppressed, as explained. Therefore one could imagine a scenario with a very light h

[1] Note also that in 2HDM-I with flavour conservation, $h \to s\bar{b}$ can be mediated at one loop. It has been shown in [32] that BR($h \to s\bar{b}$) is more than one of order of magnitude smaller than BR($h \to \gamma\gamma$).

JHEP07(2018)007

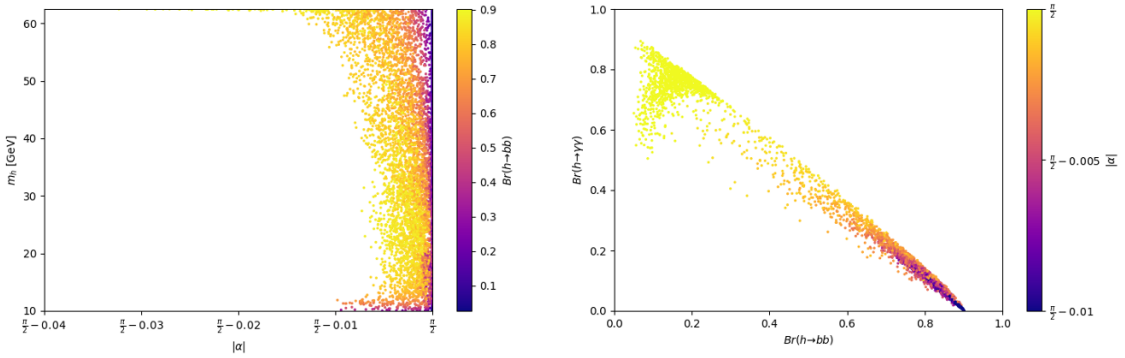

Figure 1. Left panel: BR($h \to b\bar{b}$) mapped over the ($|\alpha|$, m_h) plane. Right panel: correlation between BR($h \to b\bar{b}$) and BR($h \to \gamma\gamma$) as a function of $|\alpha|$. We assume here the 2HDM-I.

state ($m_h \ll 60\,\text{GeV}$) which has escaped LEP and Tevatron limits due to suppression in the coupling hVV. In addition, the LEP, OPAL and DELPHI collaborations have searched for fermiophobic Higgs decays through $e^+e^- \to Z^* \to Ah$ with $h \to \gamma\gamma$ and A decaying mainly into fermions and set a limit on $\sigma(e^+e^- \to Ah) \times \text{BR}(h \to \gamma\gamma) \times \text{BR}(A \to f\bar{f})$ for $m_h \in [20, 180]\,\text{GeV}$ [30, 33]. Note that this limit will depend on the coupling $ZhA \propto \cos(\beta - \alpha)$ and hence becomes weaker for $\cos(\beta - \alpha) \ll 1$. However, a very light h with $m_h \leq 60\,\text{GeV}$ is sill allowed if the CP-odd is rather heavy. We refer to [37] for more detail on these aspects. Finally, following phenomenological studies in [38, 39], CDF at Tevatron also studied $qq' \to H^\pm h$, which can lead to 4-photon final states for $H^\pm \to W^\pm h$ and $h \to \gamma\gamma$ [40], however, CDF limits are presented only for the exactly fermiophobic scenario and are not readily extendable to our more general setup.

3 Numerical results

As said previously, we are interested in the 2HDM-I for which we perform a systematic numerical scan for its parameter space. We have fixed m_H to 125 GeV and assumed that $2m_h < m_H$ such that the decay $H \to hh$ is open. The other 2HDM independent parameters are varied as indicated in table 1. We use the 2HDMC (v1.7.0) [41] public program to calculate the 2HDM spectrum as well as various decay rates and BRs of Higgs particles. The 2HDMC program also allow us to check several theoretical constraints such as perturbative unitarity, boundedness from below of the scalar potential as well as EW Precision Observables (EWPOs) which are all turned on during the scan. In fact, it is well known that EWPOs constrain the splitting between Higgs masses. In our scenario, since we ask that $m_H = 125\,\text{GeV}$ and assume $2m_h < m_H$, if we want to keep the CP-odd also light, it turns out that the charged Higgs boson would be also rather light, $m_{H^\pm} \leq 170$–$200\,\text{GeV}$ [42], as it can be seen from table 1. Moreover, the code is also linked to HiggsBounds [43] and HiggsSignals [44] that allow us to check various LEP, Tevatron and recent LHC searches.

Once in the 2HDM-I the decay channels $H \to hh$ and/or $H \to AA$ are open, the subsequent decays of h and/or A into fermions, photons or gluons will lead either to invisible H decays that can be constrained by present ATLAS and CMS data on the Higgs

JHEP07(2018)007

parameters	scan-1	scan-2	scan-3
m_H (SM-like)	125	125	125
m_h	$[10, 62.5]$	$[10, 62.5]$	$[10, 62.5]$
m_A	$[62.5, 200]$	$[62.5, 200]$	$[10, 200]$
$m_{H^\pm}$	$[100, 170]$	$[100, 170]$	$[100, 170]$
$\tan\beta$	$[2, 50]$	$[2, 50]$	$[2, 50]$
α	$\alpha{=}\pm\frac{\pi}{2} \mp \delta$	$\alpha{=}\frac{\pi}{2}$	$s_{\beta-\alpha} = [-0.35, 0.0]$
m_{12}^2	$[0, 100]$	$[0, 100]$	$[0, 100]$
$\lambda_6 = \lambda_7$	0	0	0

Table 1. 2HDM parameters scans: all masses are in GeV.

couplings. In our study, we will use the fact that the total BR of the SM-like Higgs boson into undetected BSM decay modes is constrained, as mentioned, by $\mathrm{BR}_{\mathrm{BSM}} < 0.34$ [15] where $\mathrm{BR}_{\mathrm{BSM}}$ will designate in our case the sum of $\mathrm{BR}(H \to hh)$ and $\mathrm{BR}(H \to AA)$.

In what follow, we will show our numerical results via three different scans (see table 1). These results mainly concern the $\mathrm{BR}_{\mathrm{BSM}}$, $\mathrm{BR}(H \to hh)$ and the ensuing total cross section for four photons final states which is given by

$$\sigma_{4\gamma} = \sigma(gg \to H) \times \mathrm{BR}(H \to hh) \times \mathrm{BR}^2(h \to \gamma\gamma). \tag{3.1}$$

Note that, in writing the above cross section, we have used the narrow width approximation for the SM-like Higgs state H which is justified since the total width of H is of the order of few MeV (see table 3). Furthermore, we are interested into multi-photon signatures coming from $H \to hh \to 4\gamma$ and not from $H \to AA \to 4\gamma$ decay. In the former case, in fact, because h can become totally fermiophobic, its $\mathrm{BR}(h \to \gamma\gamma)$ can in turn become maximal when $h \to Z^*A$ is not open. In the latter case, of the CP-odd Higgs state A, couplings to fermions are proportional to $1/\tan\beta$, which thus does not vanish, therefore the one loop decay $A \to \gamma\gamma$ will be suppressed compared to the tree level ones $A \to ff$ and $A \to Z^*h$.

We first show our results for $\sigma_{4\gamma}$ without imposing constraint from ATLAS searches in events with at least three photons in the final state [16]. The results of scan-1 are shown in figure 2. In this scan we only allow $H \to hh$ to be open and deviate from the exact fermiophobic limit by taking $\alpha = \pm\pi/2 \mp \delta$ where $\delta \in [0, 0.05]$. It is clear that for some values of $\delta \approx 0$, one can have an exact fermiophobic Higgs with maximal BR for $h \to \gamma\gamma$. In this scenario, The $\mathrm{BR}(H \to hh)$ can reach 17% in some cases. Thus, the four photon cross sections can become of the order of few pb when $\mathrm{BR}(h \to \gamma\gamma)$ is close to maximal and $\mathrm{BR}(H \to hh)$ large. Here, the maximum cross section is reached for $\sin(\beta - \alpha) \approx -0.06$.

The output of scan-2, which is for the exact fermiophobic limit, $\alpha = \pi/2$, is shown in figure 3. Here, we illustrate $\sigma_{4\gamma}$ as a function of $\sin(\beta - \alpha)$ in the left panel with m_h coded with different colours on the vertical axis. The $\mathrm{BR}(h \to \gamma\gamma)$ as a function of $\sin(\beta - \alpha)$ is depicted on the right panel of figure 3 with the $\mathrm{BR}(H \to hh)$ on the vertical axis. The

JHEP07(2018)007

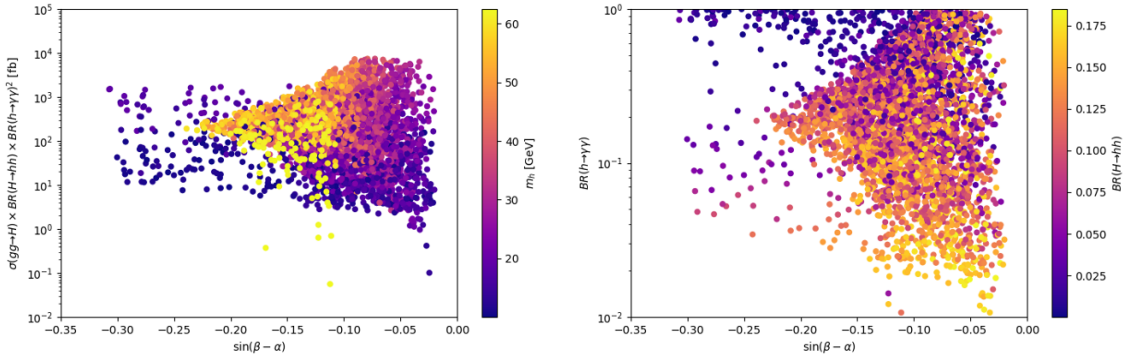

Figure 2. (Left) The $\sigma_{4\gamma}$ rate as a function of $\sin(\beta-\alpha)$ with m_h indicated on the right vertical axis. (Right) The $\mathrm{BR}(h\to\gamma\gamma)$ as a function of $\sin(\beta-\alpha)$ with $\mathrm{BR}(H\to hh)$ indicated on the right vertical axis. Both plots are for scan-1.

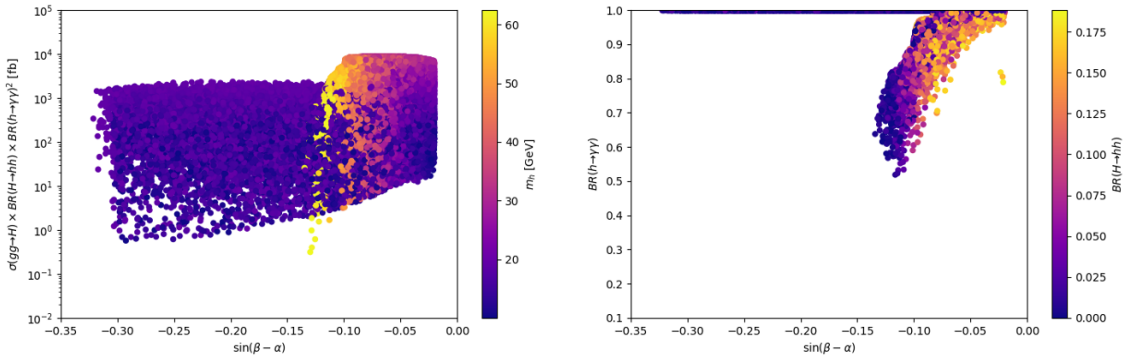

Figure 3. (Left) The $\sigma_{4\gamma}$ rate as a function of $\sin(\beta-\alpha)$ with m_h indicated on the right vertical axis. (Right) The $\mathrm{BR}(h\to\gamma\gamma)$ as a function of $\sin(\beta-\alpha)$ with $\mathrm{BR}(H\to hh)$ indicated on the right vertical axis. Both plots are for scan-2.

maximal value reached by $\mathrm{BR}(H\to hh)$ in this scenario is again around 17%. Note that, in this case of exact fermiophobic limit, only $W^\pm$ and $H^\pm$ loops contribute to the $h\to\gamma\gamma$ decay. In fact, in most cases, $W^\pm$ loop contributions to $h\to\gamma\gamma$ dominate over the $H^\pm$ ones except for small $\sin(\beta-\alpha)$, where $W^\pm$ and $H^\pm$ terms could become comparable and interfere destructively. In such a case, it may be possible that $\mathrm{BR}(h\to\gamma\gamma)$ will be suppressed and $\mathrm{BR}(h\to W^*W^*)$ slightly enhanced. This could explain the drop of the $\mathrm{BR}(h\to\gamma\gamma)$ up to 5.5×10^{-1}. Note that, for large $\sin(\beta-\alpha)\approx-0.14$, the off-shell decay $h\to V^*V^*$ can reach 3.5×10^{-1}, 1×10^{-1} for $V=W$ and $V=Z$, respectively. It is interesting to see that, in this scenario, $\sigma_{4\gamma}$ can be larger than 1 pb for a light $m_h\in[10,50]$ GeV with significant $\mathrm{BR}(h\to\gamma\gamma)$.

In scan-3, we allow $\sin(\beta-\alpha)\in[-0.35,0]$ and the CP-odd Higgs state to be as light as 10 GeV. In this case, we specifically take into account constraints from the LEP measurement of the Z width. The results are illustrated in figure 4, where we show both $\sigma_{4\gamma}$ and $\mathrm{BR}(h\to\gamma\gamma)$ as a function of $\sin(\beta-\alpha)$. Note that, for any choice of $\tan\beta$, one can tune $\sin(\beta-\alpha)$ such that α becomes $\pm\pi/2$ and then h is fermiophobic (in which case the previous discussion of scan-2 would apply again). Away from this fermiophobic limit, $\mathrm{BR}(h\to b\bar{b})$ becomes sizeable and suppresses $\mathrm{BR}(h\to\gamma\gamma)$.

JHEP07(2018)007

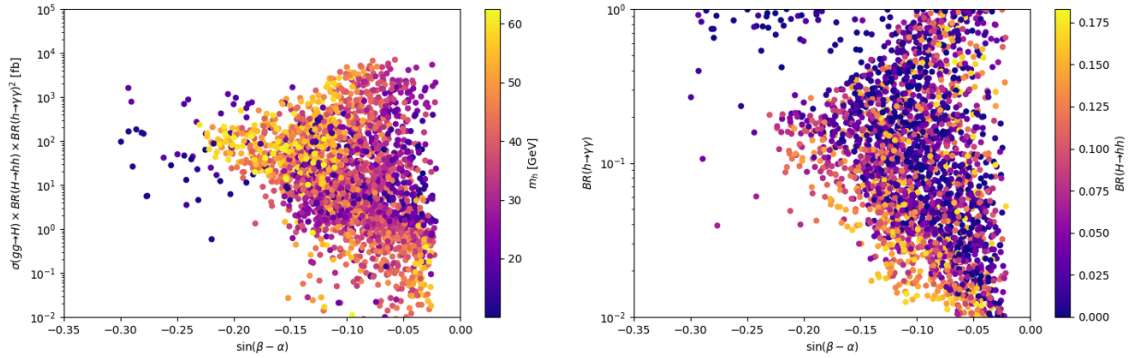

Figure 4. (Left) The $\sigma_{4\gamma}$ rate as a function of $\sin(\beta-\alpha)$ with m_h indicated on the right vertical axis. (Right) The BR($h \to \gamma\gamma$) as a function of $\sin(\beta-\alpha)$ with BR($H \to hh$) indicated on the right vertical axis. Both plots are for scan-3.

After quantifying the maximal size of the four photons cross section in the previous plots, we proceed to apply ATLAS limits coming from searches in events with at least three photons in the final state [16]. The results are shown in figure 5. The solid black line is the expected upper limit at 95% CL from ATLAS with 8 TeV centre-of-mass energy and 20.3 fb^{-1} luminosity. The green and yellow bands correspond, respectively, to a ± 1 σ and ± 2 σ uncertainty from the resonance search assumption. As it can be seen from this plot, for m_h in the $[10, 62]$ GeV range, the ATLAS upper limit on $\sigma_H \times BR(H \to hh) \times \text{BR}^2(h \to \gamma\gamma)$ is $1 \times 10^{-3}\sigma_{SM}$. We also illustrate on this figure our projection for 14 TeV using 300 fb^{-1} luminosity (based on a MC simulation that we will describe below). The dots represent our surviving points from scan-1, scan-2 and scan-3 after passing all theoretical and experimental constraints. Most of the points with significant four photons cross section and large BR($H \to hh$) and/or BR($h \to \gamma\gamma$) shown in the previous plots turn out to be ruled out by the aforementioned ATLAS upper limit [16]. It is clear from figure 5 (top-left and -right plots) that scenarios from scan-1 and scan-2 would be completely ruled out (or, conversely, be discovered) by our projection for the 14 TeV LHC run with 300 fb^{-1} luminosity while scenarios from scan-3 (bottom plot) would survive undetected. The maximal four photons cross section we obtain is of the order of 37 fb. It is interesting to note that, for scan-1 and scan-3, the remaining points still enjoy sizable BR($H \to hh$) while for the exact fermiophobic limit of scan-2 one can see from figure 5 (top-right) that the BR($H \to hh$) is less than 5×10^{-3}. This limit is much stronger than the one from invisible SM-like Higgs decays discussed previously. This can be seen in figure 6, where we illustrate the correlation between BR($H \to \gamma\gamma$) and BR($H \to hh$) for the three scans. Herein, one can verify that, for scan-1 and scan-3, BR($H \to \gamma\gamma$) and BR($H \to hh$) are anti-correlated.

Based on the results of these three scans we have selected a few Benchmark Points (BPs), which are given in table 2. These BPs can be seen in figure 5 as black stars. Note that, in BP1, both $H \to hh$ and $H \to AA$ decays are open while for the other BPs only $H \to hh$ is. For these BPs, we give in table 2 various observables such as: the total widths of h and H, Γ_h and Γ_H, respectively, BR($H \to hh$), BR($h \to \gamma\gamma$),

JHEP07(2018)007

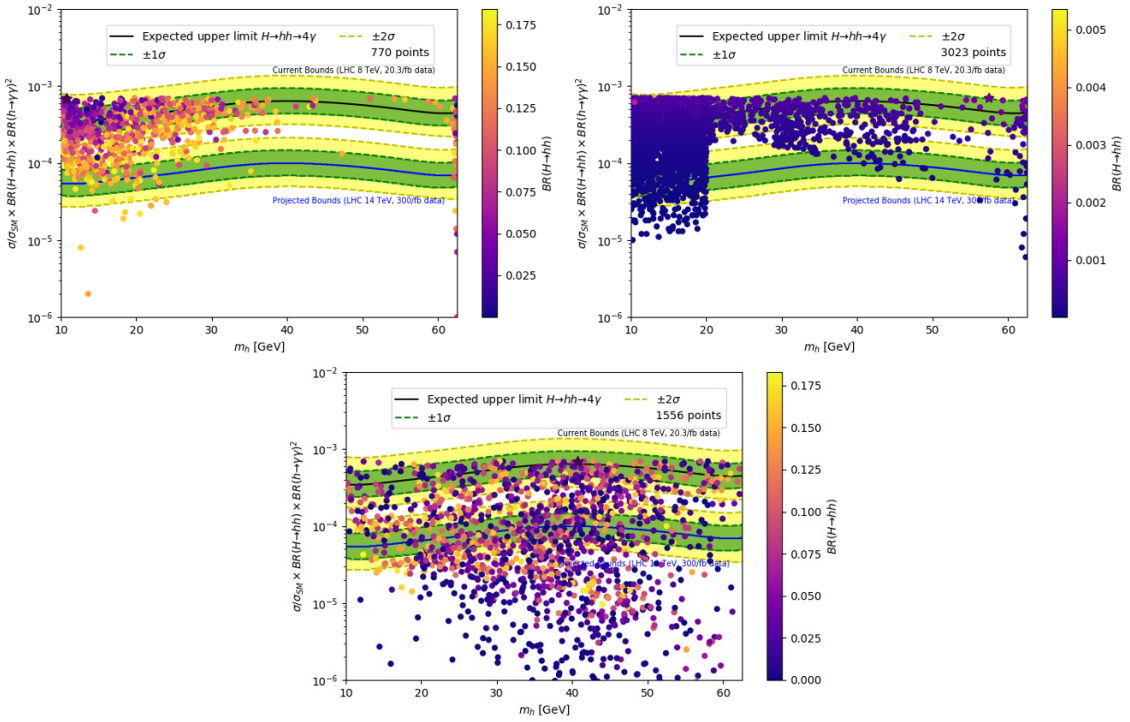

Figure 5. Upper limit at 95% CL on $\sigma_{4\gamma}$ in fb as a function of m_h and the ± 1 and ± 2 uncertainty bands resulting from ATLAS searches at 8 TeV (upper band) and our projection for 14 TeV (lower band) for (top-left) scan-1, (top-right) scan-2 and (bottom) scan-3. The dots are points that are allowed by all constraints and the black stars represent the BPs given in table 2.

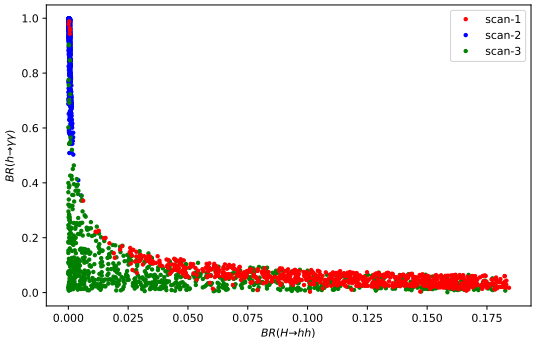

Figure 6. The correlation between BR($h \to \gamma\gamma$) and BR($H \to hh$) in the three scans.

BR($h \to Z^* A$), BR($A \to \gamma\gamma$) and the four photons cross section $\sigma_{4\gamma}$ in fb. In fact, for these BPs, we take into account all theoretical constraints as well as the LEP and LHC constraints implemented in the HiggsBounds code plus the limits from ATLAS on multi-photons final states [16], as explained in the introduction, see eqs. (1) and (2). It is also interesting to see from table 3 that the BR($A \to \gamma\gamma$) is always suppressed and cannot be used to generate multi-photon finale states. Finally, it can also be seen from this table that, even for small BR($H \to hh$) $\approx 10^{-3}$ but with maximal BR($h \to \gamma\gamma$), one can still get a large $\sigma_{4\gamma} \approx 38$ fb.[2]

[2]We provide in table 4 the allowed points after each constraint.

JHEP07(2018)007

	m_h	m_A	$m_{H^\pm}$	$\sin(\beta-\alpha)$	$\tan\beta$	m_{12}^2	Γ_h	Γ_H
BP1	10.7446	78.5676	104.8643	-0.2086	4.5840	15.8024	2.21×10^{-9}	4.679×10^{-3}
BP2	57.4401	141.1217	116.0734	-0.1147	8.6505	9.735405	5.303×10^{-9}	4.376×10^{-3}
BP3	40.6634	121.8127	161.0211	-0.0915	11.2625	22.2999	1.369×10^{-8}	4.507×10^{-3}

Table 2. Input parameters and widths corresponding to the selected BPs. All masses and widths are in GeV and for all points $m_H = 125\,\text{GeV}$.

	BR($h\to\gamma\gamma$)	BR($H\to hh$)	BR($A\to\gamma\gamma$)	BR($h\to ZA$)	BR($A\to Zh$)	$\Gamma_{Z\to Ah}$[MeV]	β'	$\sigma_{4\gamma}$ [fb]
BP1	0.1215	0.0469	7.613×10^{-5}	0.0000	0.5696	0.1890	0.00070	36.921
BP2	0.7435	0.00126	2.07×10^{-5}	0.0000	0.9488	0.0000	0.00070	35.852
BP3	0.1427	0.03348	1.23×10^{-5}	0.0000	0.9709	0.0000	0.000682	34.935

Table 3. Input parameters, BRs of CP-even and CP-odd Higgs bosons, Z boson width and four photon cross section corresponding to the selected BPs. All widths are in MeV and for all points $m_H = 125\,\text{GeV}$.

	Allowed by HiggsBounds	Allowed by theoretical constraints	Allowed by HiggsSignals	Allowed by ATLAS band	Allowed by all constraints
scan-1	49.2%	20.6%	4.5%	16.5%	0.07%
scan-2	81.6%	12.5%	61.6%	5%	0.3%
scan-3	30,6%	2.9%	27%	63%	0.15%

Table 4. Parameters as in table 3 with 10^6 points as inputs for all scans.

Before ending this section, we would like to comment on charged Higgs and CP-odd Higgs boson searches. As mentioned previously, the charged Higgs and CP-odd Higgs states are rather light in our scenarios. LHC limits on light charged Higgs states produced from top decay and decaying to $H\pm \to \tau\nu, cb$ in the 2HDM-I can be evaded by advocating the dominance of the $H^\pm \to W^\pm A$ or $H^\pm \to W^\pm h$ BRs (see [37] for more details). On the one hand, the LHC searched for a CP-odd Higgs state decaying via $A \to ZH$ [45–47] and $A \to \tau^+\tau^-$. In our scenario, the BR($A \to ZH$) will suffer two suppressions: one coming from the coupling AZH, which is proportional to $\sin(\beta-\alpha) \approx 0$, and the other one coming from the fact that $A \to Zh$ would dominate over $A \to ZH$ since h is lighter than 125 GeV and the coupling ZAh is proportional to $\cos(\beta-\alpha) \approx 1$. On the other hand, ATLAS and CMS searches for a CP-odd Higgs state decaying to a pair of τ leptons [48, 49], when applied to the 2HDM-I, only exclude small $\tan\beta \leq 1.5$ for $m_A \in [110, 350]\,\text{GeV}$ [50]. This can be understood easily from the fact that A couplings to a pair of fermions in the 2HDM-I are proportional to $1/\tan\beta$, hence both the production $gg \to A$ and the decay $A \to \tau^+\tau^-$ are suppressed for large $\tan\beta$ values. Moreover, in our scenario, BR($A \to \tau^+\tau^-$) would receive an other suppression from the opening of the $A \to Z^*h$ channel. Note also that LEP limits on a light h and a light A are implemented in the HiggsBounds code through limits on the processes $e^+e^- \to Zh$ and $e^+e^- \to hA$.

JHEP07(2018)007

4 Signal and background

As previously discussed, in figures 5–6, we have taken into account the constraints from the ATLAS collaboration reported in [1] from 8 TeV data. However, in order to project the sensitivity of the future LHC run at $\sqrt{s} = 14\,\text{TeV}$, we have to rescale these results. To determine the 'boost factors', for both signal and background processes, needed to achieve this, we resort to the MC tools. Specifically, we generate parton level events of both signal and background processes by using MadGraph 5 [51] and then pass them to PYTHIA 6 [52] to simulate showering, hadonisation and decays. We finally use PGS [53] to perform the fast detector simulations.

In order to pick out the relevant events, for our Run 1 analysis, we adopt the same selection cuts of the ATLAS collaboration given in [1], which read as follows.

- We assume $n_\gamma \geq 3$, i.e., we consider inclusive three photon events.
- The two leading photons should have a $P_t(\gamma) > 22\,\text{GeV}$ and the third one should have a $P_t(\gamma) > 17\,\text{GeV}$.
- The photons should be resolved in the range $|\eta| < 2.37$ and do not fall in the endcap region $1.37 < |\eta| < 1.52$.
- The cone separation parameter $\Delta R(\gamma\gamma)$ between a pair of photons should be larger than 0.4.

One interesting observation is that the kinematics of photons from the processes $gg \to H \to hh \to 4\gamma$ and that of $gg \to H \to AA \to 4\gamma$ are similar when $m_h = m_A$, which could be attributed to the fact that, although h and A have different parity, the differential cross sections of these two processes are both proportional to $(k_1 \cdot k_2)^2 (k_3 \cdot k_4)^2$ (plus permutations) after the sum over photon polarisations (the k_i's, for $i = 1, 2, 3, 4$, are the photon four-momenta). We provide appendix B to demonstrate the details. In figure 7, we expose the similarity between the two processes by showing some kinematic spectra of $gg \to H \to hh \to 4\gamma$ and $gg \to H \to AA \to 4\gamma$. In particular, we present the $m_{3\gamma}$ spectrum (the invariant mass of the three leading P_t-ordered photons) as well as the m_{23} spectrum (the invariant mass of the 2nd and 3rd P_t-ordered photons). Obviously, these spectra show no significant difference for these two processes $gg \to H \to hh \to 4\gamma$ and $gg \to H \to AA \to 4\gamma$, except fluctuations from numerical simulation. Therefore, the experimental methods and results of multi-photon data from $gg \to H \to AA \to 4\gamma$ can also be applied to $gg \to H \to hh \to 4\gamma$.

In order to establish LHC sensitivity to our signal process, we determine the scaling factors for both signal and backgrounds, necessary to map our own MC simulations onto the real data results of ATLAS. In doing so, we use the Leading Order (LO) cross section to determine such factors. Therefore the latter should encode the K-factors due to higher order corrections, the difference between real detector and the fast detector simulations, the mistaging rate of a jet as a photon and an electron as a photon as well, etc. In fact, when the rejection rate of a jet as a photon is considered [54], the fake rate could be around

JHEP07(2018)007

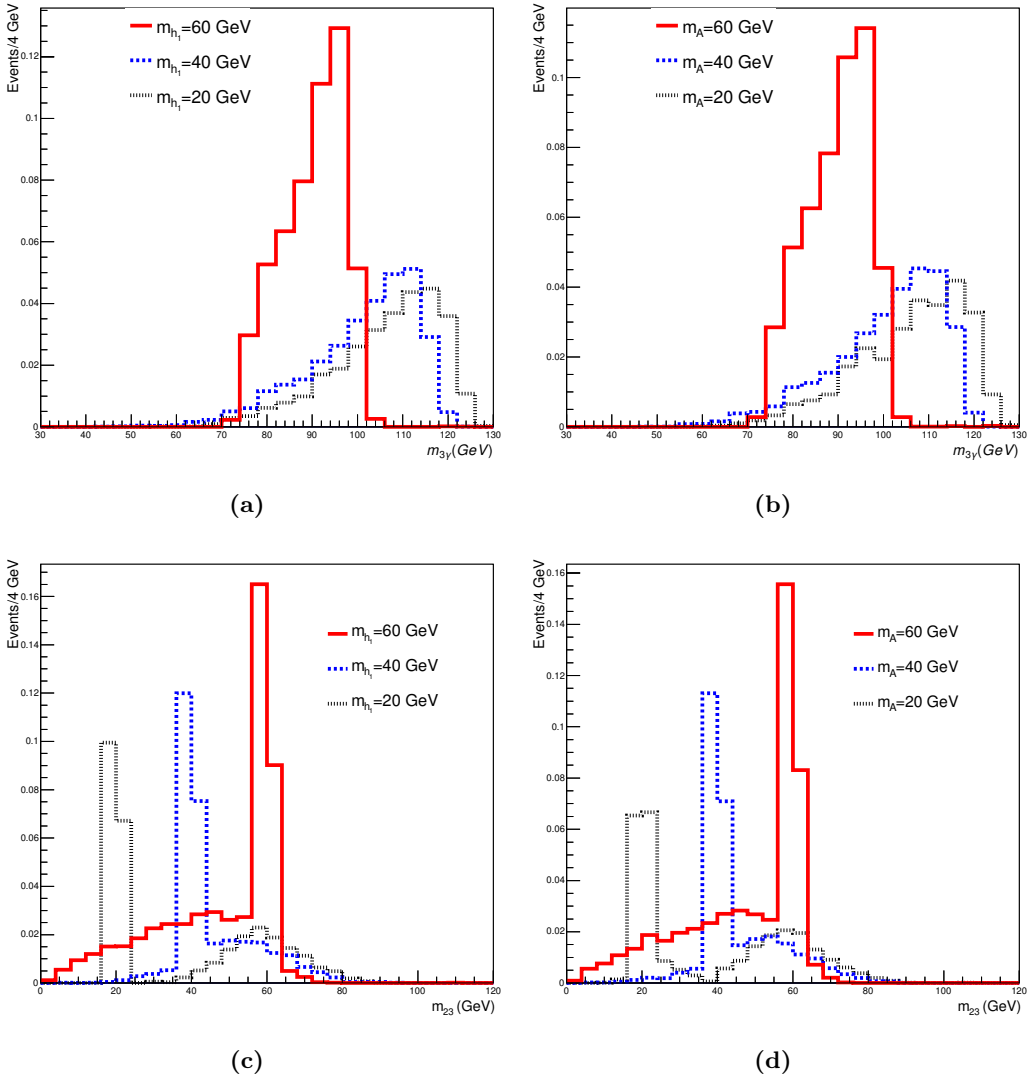

Figure 7. Distributions at detector level: (a) $m_{3\gamma}$ for $gg \to H \to hh \to 4\gamma$, (b) $m_{3\gamma}$ for $gg \to H \to AA \to 4\gamma$, (c) m_{23} for $gg \to H \to hh \to 4\gamma$ and (d) m_{23} for $gg \to H \to AA \to 4\gamma$.

10^{-3}, so for the process $\gamma\gamma + j$ the scaling factor is dominantly determined by the fake rate while for the process $\gamma + jj$ we expect the fake rate to be around 10^{-6}, the scaling factors demonstrating then that significant background contribution is indeed due to fake rates.

The scaling factors for each process are listed in table 5, as mentioned, being all determined from the aforementioned ATLAS results at 8 TeV. We also compare the experimental line-shapes with those from our MC events, which are plotted in figure 8. Although the spectra from MC are slightly harder and noticeable differences appear in the bins with $m_{3\gamma} < 50\,\text{GeV}$ and $m_{2\gamma} < 50\,\text{GeV}$, the total number of predicted events is close to the experimental ones.

By assuming the same scaling factors, we examine the boost factor in the LHC sensitivity for an increased collision energy of $\sqrt{s} = 14\,\text{TeV}$. The ensuing cross sections of the signal

JHEP07(2018)007

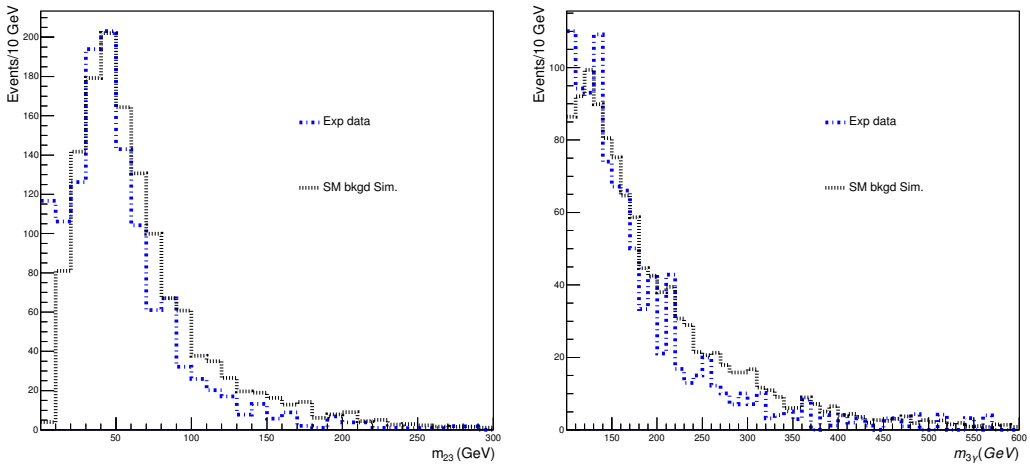

(a) **(b)**

Figure 8. The comparison of the simulated spectra of (a) m_{23} and (b) $m_{3\gamma}$ to those experimental ones is demonstrated.

process	σ with $\sqrt{s}=8$ TeV	N.o.E. (Theory)	Acc. Eff.	N.o.E. (Expected)	N.o.E. (Experimental)	Scaling factor
3γ	72.5 fb	1.47×10^3	18%	2.65×10^2	340±110	1.28
2γ	109 pb	2.21×10^6	0.4%	8.8×10^3	330±50	3.7×10^{-2}
$2\gamma+j$	58.3 pb	1.18×10^6	19%	2.24×10^5	350±50	1.56×10^{-3}
$\gamma+2j$	4.39×10^4 pb	8.91×10^8	15%	1.33×10^8	110±40	8.31×10^{-7}
γe^+e^-	5.91 pb	1.2×10^5	23.5%	2.8×10^4	89±11	3.2×10^{-3}
$2\gamma e^+e^-$	30 fb	6.1×10^2	34%	2.07×10^2	85±22	0.41
$\gamma W+X$	24.4 pb	4.95×10^5	2.9%	1.43×10^4	11.4±1.5	0.8×10^{-3}

Table 5. The scaling factors for each process of SM background are shown where N.o.E. denotes the "Number of Events" at 8 TeV when the integrated luminosity is taken as 20.3/fb and where Acc. Eff. denotes the "Acceptance Efficiency" which is determined by the selection cuts of the mentioned ATLAS analysis.

and background processes are given in table 6. Since the signal production process $gg \to H$ has a larger boost factor when the collision energy increases from 8 TeV to 14 TeV due to the larger enhancement of gluon flux, as compared to the more varied background composition, it is natural to expect a better sensitivity for the future LHC runs, as readily seen in the table. For example, when the integrated luminosity of the LHC is assumed to be 300/fb, the boost factor in cross section (which is defined in the caption) is found to be 32.2 for thew signal and 25.7 for the background. This effect reflects then in the projected sensitivities shown in figure 5 for the LHC with $\sqrt{s} = 14$ TeV and 300/fb of luminosity (blue lines).

JHEP07(2018)007

	σ with $\sqrt{s} = 8\,\text{TeV}$	σ with $\sqrt{s} = 14\,\text{TeV}$	Boost factor
Signal	$19.3 \times \beta\,\text{pb}$	$42.0 \times \beta\,\text{pb}$	32.2
Background	67.5 fb	117 fb	25.7

Table 6. The projected LHC sensitivity at 14 TeV is given, where $\beta = \text{BR}(H \to hh)\text{BR}^2(h \to \gamma\gamma)$, expressed in terms of the boost factor, defined as $\frac{\sigma(\sqrt{s}=14\,\text{TeV}) \times L_{14\,\text{TeV}}}{\sigma(\sqrt{s}=8\,\text{TeV}) \times L_{8\,\text{TeV}}}$, where $L_{14\,\text{TeV}}$ is assumed to be 300/fb and $L_{8\,\text{TeV}}$ is taken as 20.3/fb.

5 Conclusions

In this paper, we built upon previous results of some of ours, which had extracted a region of parameter space of the 2HDM-I where very light h and A states, down to 15–20 GeV or so, can be found, when the H one is assumed to be the SM-like one discovered at the LHC in 2012. This spectrum is well compatible with all standard theoretical constraints (unitarity, vacuum stability, etc.) and all available experimental data (including flavour as well as Higgs data) and thus offers the possibility of testing Higgs cascade decays of the type $H \to hh$, compatibly with the total H width extracted by global fits to the 125 GeV Higgs data. Amongst the possible decays of the h state we concentrated here upon those yielding di-photons, the overall signature then being a 4γ one, primarily induced by $gg \to H$ creation. We do so as the 2HDM-I can develop, over the aforementioned region of parameter space, a (nearly) fermiophobic limit, so that h decays into fermions (chiefly, $b\bar{b}$ and $\tau^+\tau^-$) are negligible. In fact, the availability of an ATLAS analysis performed on Run 1 samples of the LHC looking for these specific multi-photon signals allowed us, on the one hand, to validate our MC tools against the full detector environment of a multi-purpose LHC experiment and, on the other hand, to project our finding into the future by extrapolating our results to a collider energy of 14 TeV and luminosity of 300/fb. This exercise revealed that the portion of 2HDM-I parameter space where the above phenomenology is realised, while being just below the current LHC sensitivity, is readily accessible at future stages of the LHC. To confirm or disprove its existence is of paramount importance as this would almost univocally point to a specific realisation of a generic 2HDM construct as such light and fermiophobic h state cannot be realised in alternative formulations of it.

Acknowledgments

AA, RB and SM are supported by the grant H2020-MSCA-RISE-2014 no. 645722 (NonMinimalHiggs). This work is also supported by the Moroccan Ministry of Higher Education and Scientific Research MESRSFC and CNRST: Projet PPR/2015/6. SM is supported in part through the NExT Institute. RB is supported in part by the Chinese Academy of Sciences (CAS) President's International Fellowship Initiative (PIFI) program (Grant No. 2017VMB0021). Q.S. Yan and X.H. Zhang are supported by the Natural Science Foundation of China under the grant no. 11575005.

JHEP07(2018)007

A Calculation of $\Gamma(h \to b\bar{b})$ at one loop level in 2HDMs

Following the procedure in [57], at one loop order, the decay width of the Higgs boson h into $b\bar{b}$ is given by

$$\Gamma^{(1)}(h \to b\bar{b}) = \Gamma^{(0)}(h \to b\bar{b})\hat{Z}_h \left(1 - \Delta r + 2\Re\Delta M_1\right), \tag{A.1}$$

where $\Gamma^{(0)}(h \to b\bar{b})$ is the tree level width, $\hat{Z}_h$ is the finite wave function renormalisation of the external h fixed by the derivative of the renormalised self-energy and ΔM_1 is the sum of the one loop vertex diagrams and vertex counter-term $\delta(hb\bar{b})$ while Δr incoporates finite high order corrections. The computation of all one loop amplitudes and counter-terms is done with the help of the FormCalc and FeynArts packages [58–60]. Numerical evaluations of the scalar integrals are done with LoopTools [61–63]. The cancellations of ultra-violet divergences have been verified both analytically and numerically.

B The squared matrix elements of $gg \to H \to hh \to 4\gamma$ and $gg \to H \to AA \to 4\gamma$

In this appendix, we demonstrate in details that the process $gg \to H \to hh \to 4\gamma$ and the process $gg \to H \to AA \to 4\gamma$ have the same differential cross section, except an overall factors.

For the CP-even Higgs case, the matrix element of the process $gg \to H \to hh \to 4\gamma$ can be put as

$$\begin{aligned} i\mathcal{M} = {} & iC(k_1 \cdot k_2 \eta^{\mu\nu} - k_2^\mu k_1^\nu)\epsilon_\mu^*(k_1)\epsilon_\nu^*(k_2)(k_3 \cdot k_4 \eta^{\rho\sigma} - k_4^\rho k_3^\sigma) \\ & \times \epsilon_\rho^*(k_3)\epsilon_\sigma^*(k_4)\delta^{ab}\epsilon(p_1)\cdot\epsilon(p_2)\,, \end{aligned} \tag{B.1}$$

where p_1 and p_2 is the momentum of the initial gluons, $k_1 - k_4$ are momentum of 4 photons in the final state. Note that we have group the effective couplings of each vertices and the propagators together in C and just show their Lorentz structure and color indices. The squared amplitude with the average of the degree of freedom of initial states and the sum over the polarisations of photons in the final states yields

$$\begin{aligned} \overline{|\mathcal{M}|^2} = {} & \frac{1}{2}\frac{1}{2}\frac{1}{8}\frac{1}{8}\sum_{pols}\sum_{a,b=1}^{8}|\mathcal{M}|^2 \\ = {} & \frac{1}{256}|C|^2\delta^{ab}\delta_{ab}(k_1 \cdot k_2 \eta^{\mu\nu} - k_2^\mu k_1^\nu)(k_1 \cdot k_2 \eta^{\mu'\nu'} - k_2^{\mu'} k_1^{\nu'}) \\ & \times \sum_\epsilon \epsilon_\mu^*(k_1)\epsilon_{\mu'}(k_1)\sum_\epsilon \epsilon_\nu^*(k_2)\epsilon_{\nu'}(k_2)(k_3 \cdot k_4 \eta^{\rho\sigma} - k_4^\rho k_3^\sigma) \\ & \times (k_3 \cdot k_4 \eta^{\rho'\sigma'} - k_4^{\rho'} k_3^{\sigma'})\sum_\epsilon \epsilon_\rho^*(k_3)\epsilon_{\rho'}(k_3)\sum_\epsilon \epsilon_\sigma^*(k_4)\epsilon_{\sigma'}(k_4) \\ & \times \sum_\epsilon |\epsilon(p_1)\cdot\epsilon(p_2)|^2\,. \end{aligned} \tag{B.2}$$

By using the polarisation sum formula

$$\sum_\epsilon \epsilon_\mu^*\epsilon_\nu = -\eta_{\mu\nu}\,, \tag{B.3}$$

JHEP07(2018)007

and the fact $\delta_{ab}\delta^{ab} = 8$, we arrive at

$$\overline{|\mathcal{M}|^2} = \frac{1}{16}|C|^2[2(k_1\cdot k_2)^2 - k_1^2k_2^2][2(k_3\cdot k_4)^2 - k_3^2k_4^2]\,. \tag{B.4}$$

Due to the on-shell conditions for the photons of the final state, we have $k_1^2 = k_2^2 = k_3^2 = k_4^2 = 0$, then we obtain the following squared matrix element

$$\overline{|\mathcal{M}|^2} = \frac{1}{4}|C|^2(k_1\cdot k_2)^2(k_3\cdot k_4)^2\,. \tag{B.5}$$

For the CP-odd Higgs case, the matrix element of the process $gg \to H \to AA \to 4\gamma$ can be put as

$$i\mathcal{M} = iD\epsilon_\alpha^*(k_1)\epsilon_\beta^*(k_2)\epsilon^{\alpha\beta\mu\nu}k_\mu^1k_\nu^2\epsilon_\rho^*(k_3)\epsilon_\sigma^*(k_4)\epsilon^{\rho\sigma\gamma\delta}k_\gamma^3k_\delta^4\delta^{ab}\epsilon(p_1)\cdot\epsilon(p_2)\,, \tag{B.6}$$

where D includes all effective couplings and the propagators. The squared matrix element with a sum over the polarisations of photons in the final state is given as

$$\begin{aligned}
\overline{|\mathcal{M}|^2} &= \frac{1}{2}\frac{1}{2}\frac{1}{8}\frac{1}{8}\sum_{pols}\sum_{a,b=1}^{8}|\mathcal{M}|^2 \\
&= \frac{1}{256}|D|^2\delta_{ab}\delta^{ab}\sum_\epsilon\epsilon_\alpha^*(k_1)\epsilon_{\alpha'}(k_1)\sum_\epsilon\epsilon_\beta^*(k_2)\epsilon_{\beta'}(k_2)\epsilon^{\alpha\beta\mu\nu}k_\mu^1k_\nu^2 \\
&\quad\times\epsilon^{\alpha'\beta'\mu'\nu'}k_{\mu'}^1k_{\nu'}^2\sum_\epsilon\epsilon_\rho^*(k_1)\epsilon_{\rho'}(k_1)\sum_\epsilon\epsilon_\sigma^*(k_2)\epsilon_{\sigma'}(k_2)\epsilon^{\rho\sigma\gamma\delta}k_\gamma^1k_\delta^2 \\
&\quad\times\epsilon^{\rho'\sigma'\gamma'\delta'}k_{\gamma'}^1k_{\delta'}^2\sum_\epsilon|\epsilon(p_1)\cdot\epsilon(p_2)|^2 \\
&= \frac{1}{32}|D|^2\eta_{\alpha\alpha'}\eta_{\beta\beta'}\epsilon^{\alpha\beta\mu\nu}k_\mu^1k_\nu^2\epsilon^{\alpha'\beta'\mu'\nu'}k_{\mu'}^1k_{\nu'}^2 \\
&\quad\times\eta_{\rho\rho'}\eta_{\sigma\sigma'}\epsilon^{\rho\sigma\gamma\delta}k_\gamma^1k_\delta^2\epsilon^{\rho'\sigma'\gamma'\delta'}k_{\gamma'}^1k_{\delta'}^2 \\
&\quad\times\left(|\epsilon^{(+)}(p_1)\cdot\epsilon^{(-)}(p_2)|^2 + |\epsilon^{(-)}(p_1)\cdot\epsilon^{(+)}(p_2)|^2\right) \\
&= \frac{1}{16}|D|^2\epsilon^{\alpha\beta\mu\nu}k_\mu^1k_\nu^2\epsilon^{\alpha\beta\mu'\nu'}k_{\mu'}^1k_{\nu'}^2\epsilon^{\rho\sigma\gamma\delta}k_\gamma^1k_\delta^2\epsilon^{\rho\sigma\gamma'\delta'}k_{\gamma'}^1k_{\delta'}^2 \\
&= \frac{1}{16}|D|^2 2\left[(k_1\cdot k_2)^2 - k_1^2k_2^2\right]2\left[(k_3\cdot k_4)^2 - k_3^2k_4^2\right] \\
&= \frac{1}{4}|D|^2(k_1\cdot k_2)^2(k_3\cdot k_4)^2\,.
\end{aligned} \tag{B.7}$$

Since both squared amplitudes given in eq. (B.5) and eq. (B.7) are proportional to the factor $(k_1\cdot k_2)^2(k_3\cdot k_4)^2$, while the rest of factors could not lead to a significantly different kinematic dependence (except the propagators are different for these two processes where the total decay widths of h and A are different.), therefore there is no surprise to observe that the kinematics of these two processes are the same when the polarisations of photons are summed over.

JHEP07(2018)007

References

[1] ATLAS collaboration, *Combined search for the Standard Model Higgs boson using up to 4.9 fb^{-1} of pp collision data at $\sqrt{s} = 7$ TeV with the ATLAS detector at the LHC*, *Phys. Lett.* **B 710** (2012) 49 [arXiv:1202.1408] [INSPIRE].

[2] CMS collaboration, *Combined results of searches for the standard model Higgs boson in pp collisions at $\sqrt{s} = 7$ TeV*, *Phys. Lett.* **B 710** (2012) 26 [arXiv:1202.1488] [INSPIRE].

[3] H.E. Haber and D. O'Neil, *Basis-independent methods for the two-Higgs-doublet model. II. The Significance of tanβ*, *Phys. Rev.* **D 74** (2006) 015018 [hep-ph/0602242] [INSPIRE].

[4] J.F. Gunion, H.E. Haber, G.L. Kane and S. Dawson, *The Higgs Hunter's Guide*, *Front. Phys.* **80** (2000) 1 [INSPIRE].

[5] T.D. Lee, *A Theory of Spontaneous T Violation*, *Phys. Rev.* **D 8** (1973) 1226 [INSPIRE].

[6] T.D. Lee, *CP Nonconservation and Spontaneous Symmetry Breaking*, *Phys. Rept.* **9** (1974) 143 [INSPIRE].

[7] J.F. Gunion and H.E. Haber, *The CP conserving two Higgs doublet model: The Approach to the decoupling limit*, *Phys. Rev.* **D 67** (2003) 075019 [hep-ph/0207010] [INSPIRE].

[8] M. Carena, I. Low, N.R. Shah and C.E.M. Wagner, *Impersonating the Standard Model Higgs Boson: Alignment without Decoupling*, *JHEP* **04** (2014) 015 [arXiv:1310.2248] [INSPIRE].

[9] J. Bernon, J.F. Gunion, H.E. Haber, Y. Jiang and S. Kraml, *Scrutinizing the alignment limit in two-Higgs-doublet models: $m_h = 125$ GeV*, *Phys. Rev.* **D 92** (2015) 075004 [arXiv:1507.00933] [INSPIRE].

[10] P.M. Ferreira, R. Santos, M. Sher and J.P. Silva, *Could the LHC two-photon signal correspond to the heavier scalar in two-Higgs-doublet models?*, *Phys. Rev.* **D 85** (2012) 035020 [arXiv:1201.0019] [INSPIRE].

[11] J. Bernon, J.F. Gunion, H.E. Haber, Y. Jiang and S. Kraml, *Scrutinizing the alignment limit in two-Higgs-doublet models. II. $m_H = 125$ GeV*, *Phys. Rev.* **D 93** (2016) 035027 [arXiv:1511.03682] [INSPIRE].

[12] S.L. Glashow and S. Weinberg, *Natural Conservation Laws for Neutral Currents*, *Phys. Rev.* **D 15** (1977) 1958 [INSPIRE].

[13] G.C. Branco, P.M. Ferreira, L. Lavoura, M.N. Rebelo, M. Sher and J.P. Silva, *Theory and phenomenology of two-Higgs-doublet models*, *Phys. Rept.* **516** (2012) 1 [arXiv:1106.0034] [INSPIRE].

[14] H.E. Haber, G.L. Kane and T. Sterling, *The Fermion Mass Scale and Possible Effects of Higgs Bosons on Experimental Observables*, *Nucl. Phys.* **B 161** (1979) 493 [INSPIRE].

[15] ATLAS, CMS collaborations, *Measurements of the Higgs boson production and decay rates and constraints on its couplings from a combined ATLAS and CMS analysis of the LHC pp collision data at $\sqrt{s} = 7$ and 8 TeV*, *JHEP* **08** (2016) 045 [arXiv:1606.02266] [INSPIRE].

[16] ATLAS collaboration, *Search for new phenomena in events with at least three photons collected in pp collisions at $\sqrt{s} = 8$ TeV with the ATLAS detector*, *Eur. Phys. J.* **C 76** (2016) 210 [arXiv:1509.05051] [INSPIRE].

[17] N.G. Deshpande and E. Ma, *Pattern of Symmetry Breaking with Two Higgs Doublets*, *Phys. Rev.* **D 18** (1978) 2574 [INSPIRE].

JHEP07(2018)007

[18] M. Sher, *Electroweak Higgs Potentials and Vacuum Stability*, *Phys. Rept.* **179** (1989) 273 [INSPIRE].

[19] A.W. El Kaffas, W. Khater, O.M. Ogreid and P. Osland, *Consistency of the two Higgs doublet model and CP-violation in top production at the LHC*, *Nucl. Phys.* **B 775** (2007) 45 [hep-ph/0605142] [INSPIRE].

[20] I.F. Ginzburg and I.P. Ivanov, *Tree-level unitarity constraints in the most general 2HDM*, *Phys. Rev.* **D 72** (2005) 115010 [hep-ph/0508020] [INSPIRE].

[21] M.E. Peskin and T. Takeuchi, *A new constraint on a strongly interacting Higgs sector*, *Phys. Rev. Lett.* **65** (1990) 964 [INSPIRE].

[22] M.E. Peskin and T. Takeuchi, *Estimation of oblique electroweak corrections*, *Phys. Rev.* **D 46** (1992) 381 [INSPIRE].

[23] G. Altarelli and R. Barbieri, *Vacuum polarization effects of new physics on electroweak processes*, *Phys. Lett.* **B 253** (1991) 161 [INSPIRE].

[24] G. Altarelli, R. Barbieri and S. Jadach, *Toward a model independent analysis of electroweak data*, *Nucl. Phys.* **B 369** (1992) 3 [*Erratum ibid.* **B 376** (1992) 444] [INSPIRE].

[25] Particle Data Group collaboration, C. Amsler et al., *Review of Particle Physics*, *Phys. Lett.* **B 667** (2008) 1 [INSPIRE].

[26] W. Grimus, L. Lavoura, O.M. Ogreid and P. Osland, *A precision constraint on multi-Higgs-doublet models*, *J. Phys.* **G 35** (2008) 075001 [arXiv:0711.4022] [INSPIRE].

[27] W. Grimus, L. Lavoura, O.M. Ogreid and P. Osland, *The Oblique parameters in multi-Higgs-doublet models*, *Nucl. Phys.* **B 801** (2008) 81 [arXiv:0802.4353] [INSPIRE].

[28] A.G. Akeroyd, *Fermiophobic Higgs bosons at the Tevatron*, *Phys. Lett.* **B 368** (1996) 89 [hep-ph/9511347] [INSPIRE].

[29] A.G. Akeroyd, *Fermiophobic and other nonminimal neutral Higgs bosons at the LHC*, *J. Phys.* **G 24** (1998) 1983 [hep-ph/9803324] [INSPIRE].

[30] OPAL collaboration, G. Abbiendi et al., *Search for associated production of massive states decaying into two photons in e^+e^- annihilations at $\sqrt{s} = 88$ GeV to 209 GeV*, *Phys. Lett.* **B 544** (2002) 44 [hep-ex/0207027] [INSPIRE].

[31] L. Brucher and R. Santos, *Experimental signature of a fermiophobic Higgs boson*, [hep-ph/0002027] [INSPIRE].

[32] A. Arhrib, *Higgs bosons decay into bottom-strange in two Higgs doublets models*, *Phys. Lett.* **B 612** (2005) 263 [hep-ph/0409218] [INSPIRE].

[33] DELPHI collaboration, P. Abreu et al., *Search for a fermiophobic Higgs at LEP-2*, *Phys. Lett.* **B 507** (2001) 89 [hep-ex/0104025] [INSPIRE].

[34] ALEPH collaboration, A. Heister et al., *Search for $\gamma\gamma$ decays of a Higgs boson in e^+e^- collisions at $\sqrt{s}$ up to 209 GeV*, *Phys. Lett.* **B 544** (2002) 16 [INSPIRE].

[35] L3 collaboration, P. Achard et al., *Search for a Higgs boson decaying into two photons at LEP*, *Phys. Lett.* **B 534** (2002) 28 [hep-ex/0203016] [INSPIRE].

[36] D0 collaboration, V.M. Abazov et al., *Search for decay of a fermiophobic Higgs boson $h(f) \to \gamma\gamma$ with the D0 detector at $\sqrt{s} = 1.96$ TeV*, *Phys. Rev. Lett.* **101** (2008) 051801 [arXiv:0803.1514] [INSPIRE].

JHEP07(2018)007

[37] A. Arhrib, R. Benbrik, R. Enberg, W. Klemm, S. Moretti and S. Munir, *Identifying a light charged Higgs boson at the LHC Run II*, *Phys. Lett.* **B 774** (2017) 591 [arXiv:1706.01964] [INSPIRE].

[38] A.G. Akeroyd, A. Alves, M.A. Diaz and O.J.P. Eboli, *Multi-photon signatures at the Fermilab Tevatron*, *Eur. Phys. J.* **C 48** (2006) 147 [hep-ph/0512077] [INSPIRE].

[39] A.G. Akeroyd and M.A. Diaz, *Searching for a light fermiophobic Higgs boson at the Tevatron*, *Phys. Rev.* **D 67** (2003) 095007 [hep-ph/0301203] [INSPIRE].

[40] CDF collaboration, T.A. Aaltonen et al., *Search for a Low-Mass Neutral Higgs Boson with Suppressed Couplings to Fermions Using Events with Multiphoton Final States*, *Phys. Rev.* **D 93** (2016) 112010 [arXiv:1601.00401] [INSPIRE].

[41] D. Eriksson, J. Rathsman and O. Stal, *2HDMC: Two-Higgs-Doublet Model Calculator Physics and Manual*, *Comput. Phys. Commun.* **181** (2010) 189 [arXiv:0902.0851] [INSPIRE].

[42] R. Enberg, W. Klemm, S. Moretti and S. Munir, *Electroweak production of light scalar-pseudoscalar pairs from extended Higgs sectors*, *Phys. Lett.* **B 764** (2017) 121 [arXiv:1605.02498] [INSPIRE].

[43] P. Bechtle et al., HiggsBounds-4*: Improved Tests of Extended Higgs Sectors against Exclusion Bounds from LEP, the Tevatron and the LHC*, *Eur. Phys. J.* **C 74** (2014) 2693 [arXiv:1311.0055] [INSPIRE].

[44] P. Bechtle, S. Heinemeyer, O. Stål, T. Stefaniak and G. Weiglein, *HiggsSignals: Confronting arbitrary Higgs sectors with measurements at the Tevatron and the LHC*, *Eur. Phys. J.* **C 74** (2014) 2711 [arXiv:1305.1933] [INSPIRE].

[45] ATLAS collaboration, *Search for a CP-odd Higgs boson decaying to Zh in pp collisions at* $\sqrt{s} = 8$ *TeV with the ATLAS detector*, *Phys. Lett.* **B 744** (2015) 163 [arXiv:1502.04478] [INSPIRE].

[46] CMS collaboration, *Searches for a heavy scalar boson H decaying to a pair of 125 GeV Higgs bosons hh or for a heavy pseudoscalar boson A decaying to Zh, in the final states with* $h \to \tau\tau$, *Phys. Lett.* **B 755** (2016) 217 [arXiv:1510.01181] [INSPIRE].

[47] CMS collaboration, *Search for a pseudoscalar boson decaying into a Z boson and the 125 GeV Higgs boson in* $\ell^+\ell^- b\bar{b}$ *final states*, *Phys. Lett.* **B 748** (2015) 221 [arXiv:1504.04710] [INSPIRE].

[48] ATLAS collaboration, *Search for neutral Higgs bosons of the minimal supersymmetric standard model in pp collisions at* $\sqrt{s} = 8$ *TeV with the ATLAS detector*, *JHEP* **11** (2014) 056 [arXiv:1409.6064] [INSPIRE].

[49] CMS collaboration, *Search for neutral MSSM Higgs bosons decaying to a pair of tau leptons in pp collisions*, *JHEP* **10** (2014) 160 [arXiv:1408.3316] [INSPIRE].

[50] A. Arhrib, K. Cheung, J.S. Lee and C.-T. Lu, *Enhanced charged Higgs production through W-Higgs fusion in W-b scattering*, *JHEP* **05** (2016) 093 [arXiv:1509.00978] [INSPIRE].

[51] J. Alwall et al., *The automated computation of tree-level and next-to-leading order differential cross sections and their matching to parton shower simulations*, *JHEP* **07** (2014) 079 [arXiv:1405.0301] [INSPIRE].

[52] T. Sjöstrand, S. Mrenna and P.Z. Skands, *PYTHIA 6.4 Physics and Manual*, *JHEP* **05** (2006) 026 [hep-ph/0603175] [INSPIRE].

JHEP07(2018)007

[53] J. Conway, http://conway.physics.ucdavis.edu/research/software/pgs/pgs4-general.htm.

[54] http://atlas.web.cern.ch/Atlas/GROUPS/PHYSICS/TDR/access.html.

[55] OPAL collaboration, G. Abbiendi et al., *Flavor independent h0A0 search and two Higgs doublet model interpretation of neutral Higgs boson searches at LEP*, *Eur. Phys. J.* **C 40** (2005) 317 [hep-ex/0408097] [INSPIRE].

[56] OPAL collaboration, G. Abbiendi et al., *Two Higgs doublet model and model independent interpretation of neutral Higgs boson searches*, *Eur. Phys. J.* **C 18** (2001) 425 [hep-ex/0007040] [INSPIRE].

[57] A. Arhrib, R. Benbrik, J. El Falaki and W. Hollik, *Triple Higgs coupling effect on $h^0 \to b\bar{b}$ and $h^0 \to \tau^+\tau^-$ in the 2HDM*, *Phys. Lett.* **B 774** (2017) 195 [arXiv:1612.09329] [INSPIRE].

[58] T. Hahn, *Generating Feynman diagrams and amplitudes with FeynArts 3*, *Comput. Phys. Commun.* **140** (2001) 418 [hep-ph/0012260] [INSPIRE].

[59] T. Hahn and M. Pérez-Victoria, *Automatized one loop calculations in four-dimensions and D-dimensions*, *Comput. Phys. Commun.* **118** (1999) 153 [hep-ph/9807565] [INSPIRE].

[60] T. Hahn and M. Rauch, *News from FormCalc and LoopTools*, *Nucl. Phys. Proc. Suppl.* **157** (2006) 236 [hep-ph/0601248] [INSPIRE].

[61] G.J. van Oldenborgh, *FF: A Package to evaluate one loop Feynman diagrams*, *Comput. Phys. Commun.* **66** (1991) 1 [INSPIRE].

[62] T. Hahn, *Loop calculations with FeynArts, FormCalc and LoopTools*, *Acta Phys. Polon.* **B 30** (1999) 3469 [hep-ph/9910227] [INSPIRE].

[63] T. Hahn, *Feynman Diagram Calculations with FeynArts, FormCalc and LoopTools*, PoS(ACAT2010)078 [arXiv:1006.2231] [INSPIRE].

JHEP07(2018)007